



# Challenges in sample preparation for measuring nanoparticles size by scanning electron microscopy from suspensions, powder form and complex media

Najoua Bouzakher Ghomrasni, Carine Chivas-Joly, Laurent Devoille,  
Jean-François Hochepied, Nicolas Feltin

## ► To cite this version:

Najoua Bouzakher Ghomrasni, Carine Chivas-Joly, Laurent Devoille, Jean-François Hochepied, Nicolas Feltin. Challenges in sample preparation for measuring nanoparticles size by scanning electron microscopy from suspensions, powder form and complex media. Powder Technology, 2020, 359, pp.226 - 237. 10.1016/j.powtec.2019.10.022 . hal-03488507

HAL Id: hal-03488507

<https://hal.science/hal-03488507>

Submitted on 21 Dec 2021

**HAL** is a multi-disciplinary open access archive for the deposit and dissemination of scientific research documents, whether they are published or not. The documents may come from teaching and research institutions in France or abroad, or from public or private research centers.

L'archive ouverte pluridisciplinaire **HAL**, est destinée au dépôt et à la diffusion de documents scientifiques de niveau recherche, publiés ou non, émanant des établissements d'enseignement et de recherche français ou étrangers, des laboratoires publics ou privés.



Distributed under a Creative Commons Attribution - NonCommercial 4.0 International License

# Challenges in sample preparation for measuring nanoparticles size by scanning electron microscopy from suspensions, powder form and complex media

Najoua Bouzakher Ghomrasni<sup>1</sup>, Carine Chivas-Joly<sup>1</sup>, Laurent Devoille<sup>1</sup>, Jean-François Hochepied<sup>2</sup>, Nicolas Feltin<sup>1</sup>

<sup>1</sup>*LNE, 29 Avenue Roger Hennequin, 78197 Trappes Cedex, France*

<sup>2</sup>*ENSTA ParisTech – UCP, 1024 Boulevard des Maréchaux, 91762 Palaiseau Cedex (France)*

Corresponding author: carine.chivas-joly@lne.fr

Email address: carine.chivas-joly@lne.fr- Telephone number: +33130691072

## Abstract

Commercial products containing nanomaterials are already a part of our everyday life. The dimensional parameters play an important role for identifying nanoparticles. Various techniques are available for measuring the particles size and shape. However, electron microscopy-based techniques are often considered as the preferred methods for characterizing their dimensional properties. Samples preparations remain a key step but no standardized protocol is currently available. Scanning electron microscopy measurements require well-dispersed particle population corresponding to a statistically representative sample. This work presents a new approach, to prepare samples based on spincoating technique in order to measure in a reliable manner the constituent particle size. This method consists of three key processing steps: (i) extraction from complex media, (ii) redispersion by means of probe sonication and (iii) deposition by spincoating. The approach combines several factors such as pH, zeta potential, duration, concentration, sonication and spin coater parameters, that can influence agglomeration state of nanoparticles.

**Key words:** Nanoparticles, Probe-sonicator, Spin Coating, Scanning electron microscopy, Zeta potential, Metrology

## **Introduction**

Incorporation of nanoparticles in commercial products has been increasing for the past 15 years[1] and nowadays their life cycle raises some societal issues about possible environmental and human health consequences due to particles release [2]. In the fringes of this industrial development, many regulatory and government agencies ask for a reliable risk assessment related to the exposure of the citizens to nanomaterials.

According to the European Commission, a nanomaterial is defined as a “natural, incidental, or manufactured material containing particles”, in an unbound state (isolated particles) or as an aggregate (a particle comprising of strongly bound or fused particles) or as an agglomerate (a collection of weakly bound particles or aggregates where the resulting external surface area is similar to the sum of the surface areas of the individual components) and where, for 50% or more of the particles in the number size distribution, one or more external dimensions is in the size range 1–100 nm” (European Commission,[3]). Consequently, the nano character of a substance is determined by establishing the number-weighted particle size distribution, whatever they are isolated particles or constituent particles of agglomerates and or aggregates. Measuring the size of constituent particles in commercial products becomes a major challenge.

Furthermore to assess the emerging risk linked to the nanoparticle dissemination, ISO/TC 229, the technical committee in charge of nanomaterials for international standardization, proposed a list of parameters for a better physico-chemical characterization and identification of engineered nanoscale materials (ISO/TR 13014:2012 [4]). The objective is to give an exhaustive and accurate description of particles based on a reliable characterization of these physico-chemical properties.

In this list, we can find the dimensional properties such as size, size distribution, shape and agglomeration/aggregation state. Various instrumental techniques are available for measuring the particles dimensional properties but the most reliable ones are the microscopy-based direct techniques: AFM (Atomic Force Microscopy), TEM (Transmission Electron Microscopy) and SEM (Scanning Electron Microscopy). Imaging techniques are classified as direct techniques because they involve a direct observation of the nanoparticle dimensions and provide a measurement of the “geometrical” size directly linked to the SI length unit, the meter. That is the reason why these imaging techniques represent powerful tools for characterizing the nanoparticle size, the size distribution as well as the shape of the nanoparticles.

In SEM techniques, the dimensional parameters can be expressed in terms of projected area equivalent diameter corresponding to the diameter of a sphere with the same projected surface as the investigated particle. The mean, median or modal values of this measurand are deduced from a histogram of size distribution graphically represented from the observation and counting of individual and constituent particles.

However, in the context of identification of nanomaterials, as with many sizing methods, the sample preparation is a key step of the measuring process and requires a great amount of work for minimizing the agglomeration state, which impacts negatively the measurement result of constituent nanoparticles. Indeed, individualisation of particles on the substrate makes it possible to reduce significantly the measurement errors. The measurements generated by automatic routines or software implemented during the step of image analysis process and performed only on isolated particles are more reliable compared with measurements carried out within agglomerates because the contour of each particle is more noticeable. Furthermore, EM specimen must be statistically representative of the studied suspension/powder. Sometimes measuring a nanoparticle population in powder form is not possible - even with sophisticated image processing softwares - because of the too strong agglomeration/aggregation between nanoparticles. Consequently, the powder form containing particles must be previously suspended in a specific liquid medium. Achieving a stable particle suspension is the first crucial step. For that purpose, different suspension methods can be found in the literature and the effects of various parameters (concentration, solvent nature, pH, particle surface charge) or devices (ultra-sonication bath or probe) have been investigated [5].

For instance, the application of ultrasound is often necessary to break up the agglomerates within the suspension. But, an uncontrolled sonication method can induce processes of re-agglomeration of nanoparticles [6][7]. The specific energy input is commonly identified as the main factor to separate agglomerates into constituent particles [6][8][9]. In several papers, for improving dispersion and suspension stability, the authors combine sonication and modification of the particles surface charge by changing pH. For example Mandzy et al. [7], have studied the breakage of commercial TiO<sub>2</sub> agglomerated particles in aqueous suspension while controlling zeta potential at constant ionic strength. In colloids, zeta potential is the electric potential at the slipping plane and due to the separation of charges in the electric double layer. It is linked to the surface electrical charge of particles in water suspension [10]. Controlling zeta potential depending on the pH makes it possible to stabilize the suspension by maximizing Coulomb interactions (repulsion) between particles. But, this study has shown that an optimal power should be also found to well disperse the particles and above this threshold the reduction of agglomeration is negligible or in some cases a re-agglomeration [6] of nanoparticles occurs. Jiang et al [11] obtained similar results with TiO<sub>2</sub> (P25) nanoparticles by changing pH and sonication conditions.

In some cases, the amount of nanoparticles in colloidal suspension is also a critical point because high concentration can lead to an increase of the inter-particle collision frequency favouring their partial agglomeration (in absence of repulsive forces), whereas a too low concentration would make the microscopy measurements particularly fastidious. An optimal concentration is required to have a good dispersion allowing direct measurement in a reasonable time.

But, even if the obtained suspension sample (particles in liquid) is stable, the air-drying of a suspension droplet deposited on a substrate leads unavoidably to an agglomeration process. During the last fractions of second of drying, the capillary forces tend to agglomerate nanoparticles when they are still partially immersed [12][13]. The use of a spin-coater is a good way to prevent capillary force from acting [14].

Hoo et al. [15] detailed influence parameters such as solvent, pH, concentration or substrate nature and compared two different deposition methods involving either a spin-coater or a specific fluid cell for an optimal dispersion of particles on a substrate before AFM measurements. A similar method based on a spin-coater was proposed for depositing silica nanoparticles on two substrates with different behaviours: the mica sheet, an insulating material with a hydrophilic surface and the silicon wafer, conductor and hydrophobic [14]. The protocol consists of two steps, (i) the spreading of the particles stable suspension on the surface at low rotation speed and (ii) a rapid drying at high speed. The surface density of nanoparticles can be controlled by parameters of the first step (rotation speed and duration).

Mica sheet cannot be used for analysing nanoparticles by SEM because its insulating nature can induce damages when nanoparticles are submitted to electron beam irradiation [14]. The silicon wafer is more suitable but the SiO<sub>2</sub> layer at the interface is negatively charged like most of metallic or oxide nanoparticles (at neutral pH). So, NP/substrate interactions induce repulsion forces minimizing the nanoparticle adhesion on the surface. To remedy this problem, the substrate can be functionalized with poly-L-lysine or amino-ethane-thiol that are capable of significantly improving the attachment of isolated nanoparticles through electrostatic interactions [16]. However, these kinds of coating can deteriorate the surface features and disrupt the measuring process [14].

A few review papers [17][18] have discussed on the preparation methods and stability of the suspension. Recent studies focus only on indirect measurements without tackling the microscopy-based technique case [19][20]. Bibliography reveals information is lacking and protocols are non-homogeneous [21][22][23][24]. The objective of this study is to propose a universal approach for the sample preparation of particulate materials suitable for microscopy technique whilst taking into account the results already published in literature. The development of uniform metrological procedure is essential for sample preparation to assess to the constituent particle size distribution. Based on a reasoned approach combining various factors (pH, zeta potential, temperature, duration and power of sonication, concentration, and spin coater parameters), our objective is to develop a new methodology to prepare sample and to establish a reliable measurement of size distribution by SEM of particles from various sources.

The proposed protocol has been developed and tested on four samples of particulate materials representative of manufacturing products potentially present in the market [25].

Three materials were supplied as powders (SiO<sub>2</sub>, CeO<sub>2</sub> and TiO<sub>2</sub>) and one was incorporated in a consumer product (Food-grade TiO<sub>2</sub> in a complex medium) and has to be extracted before deposition on the substrate.

## **Materials and methods**

### ***Materials***

Four kinds of particles have been investigated with different types of chemical composition, structure (colloidal suspension, powder form), and morphology coming from various sources (e.g. commercial, manufactured or synthetized in laboratory).

The food-grade TiO<sub>2</sub> (referred to as E171) used in a variety of food products (candies, chewing-gums, industrial cheeses,...) as a white colouring agent [26] or the field of drugstore or pharmacy (including Doliprane® or toothpaste ) have constituent particle number-weighted average sizes closed to 106 and 145 nm and with the a number-weighted size distribution range between 30 and 300 nm [27][28]. TiO<sub>2</sub> particles can be found in cosmetics or varnishes as UV absorber. In this case their optically transparent with constituent particle sizes around 20 nm.

Amorphous Silica (SiO<sub>2</sub>) nanoparticles are used in various areas such as, in cosmetic products, food (additive E151), automotive industry, paints... Additive E151 is employed as anticaking agent, antifoaming agent or flow aid in powdered food.

Cerium oxide nanoparticles (CeO<sub>2</sub>) are widely used in fuel additives, polishing agents, catalysts, heat stabilizers, microelectronics, and nanomedicine [29][30].

### ***Sample preparation***

A titanium dioxide (anatase-type as raw material) (TiO<sub>2</sub>) particles (mentioned TiO<sub>2</sub>-Lab), was prepared by a hydrolysis process of a mixture of titanium (IV) butoxide and triethanolamine under microwave heating as described by Marchetti 2013 [31]. A cerium oxide (CeO<sub>2</sub>) powder (mentioned CeO<sub>2</sub>-Lab) has been obtained by heating a cerium (III) nitrate in an ammoniac or soda medium [32]. A commercial food product containing TiO<sub>2</sub> nanoparticles have been chosen in solid form. TiO<sub>2</sub> particles (noted TiO<sub>2</sub>-Food) have been extracted and isolated from the solid sample of the chewing-gum (Freedent®). A commercial sample of silica nanoparticles has been supplied in powder form (Tixosil 43 noted SiO<sub>2</sub> precipitated synthetic amorphous silica due to the manufacturing process).

The powder form of the different samples was suspended in ultrapure water and carried out in several steps. The steps differ for the nanoparticles without matrix (e.g. pristine nanoparticles synthetized or commercial powder form) and nanoparticles with matrix (e.g. nanoparticles embedded in food).

- For nanoparticles in powder form, 0.1 g was dispersed in 10 ml of ultrapure water. The suspension was sonicated in a bath 20 min to improve the redispersion of the particles.
- For nanoparticles in food matrix such as chewing gum, only one part was extracted from the food, the coating of the chewing gum containing TiO<sub>2</sub>. This step corresponds to suspension of five chewing-gums plunging in 10 mL of ultra-pure water. Then, in order to remove the sugar included in

the coating, the white suspension is washed 5 times by following a three-step protocol. The first step was the centrifugation (Sovrall ST8 centrifuge) at 4 500 rpm (3 260 x g) during 20 minutes. According to several authors [28][33], the size of TiO<sub>2</sub> nanoparticles used in food is around 130 nm. Consequently, a rotation speed of 4 500 rpm (3 260 x g) is sufficient to separate the solid phase from the liquid phase.

- The second step was the replacement of the supernatant liquid by ultra-pure water. This step must be carried out as quickly as possible to avoid the redispersion of the smallest nanoparticle fraction. Choice of the solvent is crucial: an efficient washing needs residues to be soluble in the solvent. The last step was the sonication with an ultrasonic bath to re-suspend the particles in the solvent.

## **Methods**

### **a) Desagglomeration step by ultra-sonication**

The dispersion of particles in a solvent (e.g. ultra-pure milliQ water) is a crucial step and the sonication method is widely used in laboratory in order to break the agglomerates naturally occurring in the particles colloidal suspension. In this study, the ultrasonication was conducted using a Vibracell 75043 Ultrasonifier (750 W, 20 kHz, Fischer Bioblock Scientific, 13 mm horn). The dispersions were sonicated in a cold-water bath maintained at a constant temperature. Calorimetric energy density (J/mL) was calculated as a function of input power, time and dispersion volume. The energy densities required in our sonication process is similar to previously published work [7][34], which demonstrates that the power delivered to the suspensions is 378 and 1 667 J/mL. The power is the main parameter to separate agglomerates into primary particles. To achieve a stable dispersion of nanoparticles, we started with guidelines developed in the framework of the European project NANOREG [35], and in parallel we have examined the feasibility of maximum dispersion by probe sonication for suspensions of pyrogenic powders and incorporated recommendation previously published in earlier literature [34]. Recent studies led by Retamal Marín et al [36] underline that the energy density is the main parameter for sample preparation based on ultrasonication probe for suspension of various pyrogenic powders. Power applied on ultrasonication probe (with a separate vial) is not the only one parameter to obtain sample homogeneity and to achieve a minimal state of agglomeration.

To go in depth, and to control the dispersion and the stability process, it's important to study how different parameters such as the pulse and the time duration can affect the dispersion and need to be adjusted to obtain a stable colloidal suspension. This approach was tested and optimized in NANOMET project [37] as followed: each suspension has been sonicated with a probe-sonicator (20 minutes with cycles of 10 seconds ON with amplitude of 20% and 30 seconds OFF), that correspond to sonication energy at 378 J/mL. The erosion of the used ultrasonic probe may induce contaminations of the sample. In order to avoid contaminating the suspension with pieces of metal or metallic oxide due to probe erosion, this latter is not

directly immersed in the suspension. A plastic tube filled with the particle suspension is placed in a bath containing the probe. Consequently, the suspension is totally protected from the probe contamination. Furthermore, during sonication step, the suspension temperature may dramatically increase, which may lead to aggregation between NP in some cases. For this reason, the bath with the probe and the tube is constantly cooled with ice.

**b) Method of deposition by spin-coating**

A droplet of particle colloidal suspension is deposited on the centre of the silicon wafer substrate and put on the spin coater. The spin coater used is a LabSpin 6 SUSS Microtec. The recommended protocol for getting a good dispersion of particles on the substrate consists in two steps [14][38]. The first step is the spreading phase, where the rotational speed is fixed at 1000 rpm/min with a 500 rpm/min<sup>2</sup> acceleration if the solvent is aqueous, and 300 rpm/min if the solvent is more volatile (ethanol, acetone ... ) during 60 seconds. The second step is the drying phase with a rotational speed fixed at 8000 rpm/min during 10 seconds.

The performance of this method depends on the ability of particles to adhere to substrate. But, most of particles (metal or metal oxide) are generally negatively charged on surface like the silicon substrate commonly used. Consequently, two ways to promote an efficient attachment between particle and substrate are proposed in this study: (i) modifying the particle surface charge by changing pH of the medium or (ii) functionalizing the substrate surface with Poly-L-Lysine (PLL). This molecule is positively charged at each end and form a bridge between particle and substrate. To prepare a substrate functionalized with PLL, the silicon wafer is immersed during 30 min in Poly-L-lysine (PLL) suspension with a concentration fixed at 0.1 g/L. The choice between the both approaches (i) and (ii) depends on the isoelectric point (IEP) of the considered particles as shown in the “results and discussion” section.

**c) SEM image acquisition and data analysis with statistical tools**

SEM images have been performed with a Zeiss ULTRA-Plus equipped of a Field Emission Gun (FEG) microscope and in-Lens SE detector. The provider claims that the resolution of this microscope is roughly 1.7 nm at 1kV and 1.0 nm at 15 kV (for a working distance, WD, close to 2 mm). All images have been carried out through secondary electrons collected by InLens detector. From images, the particle area-equivalent diameter,  $D_{\text{area-eq.}}$ , is determined and this measurand is defined as the diameter of a sphere that would have a projected surface similar to the projected image of particles to be measured. Image analysis processing has been performed with a specific semi-automatic routine Software [39][14]. This program enables the user to measure and count the constituent particles through control interface.

The mean, modal and median diameters and number-weighted size distribution are estimated using a well-known statistical method: the Maximum-Likelihood estimation. The principle is to estimate the parameters

of a theoretical probability distribution from the information conveyed by the different single particles considered in the SEM image. However, prior to the estimation process, a choice has to be made regarding the theoretical probability distribution which would be suitable to represent the size distribution. The histograms obtained on a given sample are very informative to this extent and Gaussian distributions or Log-Normal distributions often seem to be a good choice, whatever the material considered [40]. Of course, the mean, modal and median diameters could be determined directly from particle count data without going through the stage of histogram construction. But, this is a precaution to identify a multimodal population or the eventual presence of a shoulder on the main mode characterizing a second mode.

#### *d) DLS measurements*

The hydrodynamic mean diameter of particles ( $D_{hd}$ ) was measured by Dynamic Light Scattering (DLS) with a Zetasizer Nano ZS from Malvern equipped with a Helium-Neon laser (4 mW - 632.8 nm). Particle size was measured by collecting the scattered light with a detector located at 173°. Around 1 mL of sample was deposited onto the cell as dispersion and was irradiated by a laser. The hydrodynamic diameter value corresponds to the number weighted mean diameter of nanoparticles surrounded by an ionic layer in the suspension determined by the NNLS method. This latter is an algorithm specifically developed for polydispersed particles populations and regarding actual case seems always closer to SEM equivalent diameter than the Z-average parameter. In fact, the cumulant method (z-average) yields the harmonic mean of the intensity-weighted size distribution, while the NNLS method is more consistent with SEM measurement. Six specimens were prepared with dilutions factors (x10, x20, x50, x100, x200, and x500). Each suspension has been sonicated by following the protocol described in Methods section. The use of probe sonication is in accordance with the majority of dispersion studies [34][36][41][42]. In DLS technique, the random changes in the intensity of scattered light measured by the instrument are due to Brownian movement of NP in the liquid. From these intensity fluctuations, a diffusion coefficient is then evaluated and a hydrodynamic diameter,  $D_{hd}$ , is finally deduced from the Stokes-Einstein relationship. But, if the suspension is too concentrated (low dilution factors), the signal is negatively impacted by the multiple scattering phenomenon wherein the photons are scattered multiple times by the sample before being collected by the detector. As a result the  $D_{hd}$  measured value will be incorrect. In contrast, if the suspension is too diluted (large dilution factors) the signal to noise ratio is too bad and the measured  $D_{hd}$  values dramatically increase. Between these both situation, this curve exhibits a range of dilution factors where ( $D_{hd}$ ) reaches a plateau [43]. Then, we choose a concentration of the suspension corresponding to  $D_{hd}$  defined by this plateau to ensure reliable values.

### e) Zeta potential measurements

For each sample, the measurement of zeta potential at initial pH of the colloidal suspension was carried out. The presence of charged sites at the surface of nanoparticles immersed in an electrolytic suspension strongly impacts the spatial distribution of ionic species in their surroundings. Due to this surface charge, nanoparticles tend to attract ions with an opposite charge and inversely repel ions of same charge in the suspension. As a result, the interface nanoparticle/suspension consists of two different layers. The stern layer is formed by a compact layer of ions strongly linked to the particle surface and a diffuse layer located between stern layer and bulk suspension. The zeta potential corresponds to the theoretical electric potential difference between the potential occurring at the slipping plane of this double ionic layer and a null reference potential at infinity. The slipping plane is usually defined as the interface where the Stern and diffuse layers meet.

The zeta potential is linked to the charge of particles in a colloidal suspension and an indicative parameter of the stability of this suspension. It depends on the nature of the dispersion medium and the physico-chemical properties of the nanoparticles (size, shape, concentration, chemical composition) [44]. The value of the zeta potential is also related to the ionic strength of the suspension. Increasing the ionic strength induces a compression of the electric double layer and decreases the zeta potential of the nanoparticles [10].

Typically, the higher the zeta-potential is, the more stable the colloid is. Even if it is difficult to generalize, in the case of metal oxide nanoparticles such as TiO<sub>2</sub>, SiO<sub>2</sub> or CeO<sub>2</sub> in aqueous suspensions, the stability areas of colloidal suspensions formed by charged particles can be typically achieved by zeta potentials higher than 30 mV in absolute value [45][46][47]. The stability of a colloidal suspension can be also achieved by providing steric interactions between particles. In this case, the particles are functionalized with a polymer layer for instance. But, for our purpose, this approach is not chosen because the size of particles is artificially increased and their real dimension impossible to be accurately determined.

The range from -15 mV and 15 mV typically represents an area where the agglomeration process begins to occur. When the zeta-potential is equal to zero (Isoelectric Point, IEP), the agglomeration will be maximum and all agglomerates will precipitate. In this study, the zeta potential measurements were carried out for assessing the stability of NP in the suspensions. The measurements were performed by using the Zetasizer Nano ZS by keeping constant the ionic strength in all the pH range investigated. The physical principle of the used technique is the Electrophoretic Light Scattering (ELS). Then, a set of suspensions at different pH have been prepared by adding few amounts of acid (perchloric acid) or base (NaOH) in an aqueous suspension of nanoparticles made by diluting the originate suspension in ultra-pure Milli-Q water. The ionic strength (0.1 M) has been maintained constant over the whole set of prepared suspensions by adding sodium perchlorate in the suspensions. Note that sodium and perchlorate ions seem to be indifferent to the metal

oxide surface investigated here because no shift of IEP has been observed. Each suspension has been sonicated with the protocol described above prior to zeta potential measurements.

## Results and discussion

Before depositing a droplet of colloidal suspension composed of nanoparticles onto a substrate, the first step is to ensure that the suspension is stable and the particles are well-dispersed. Applying sonication techniques for breaking the agglomerates potentially present can be effective but only when the repulsive interaction forces between nanoparticles are sufficiently strong to prevent re-agglomeration. As detailed in the previous section, the stability electrostatically obtained depends especially on zeta potential value. Then firstly, each suspension has been sonicated by following the protocol described in Material and Method section.

The dependency of the zeta potential on the pH reflects the electric properties of the particle surface in acidic and alkaline media, of course on condition that particles are not soluble: the solubility of titania or ceria is very low in our considered pH range (2-12), silica begins to dissolve at pH>10. The  $\zeta$ -curves of TiO<sub>2</sub>-Lab, CeO<sub>2</sub>-Lab, SiO<sub>2</sub> and TiO<sub>2</sub>-Food have therefore been built at constant ionic strength (Figure 1).

The isoelectric points for TiO<sub>2</sub>-Lab and for CeO<sub>2</sub>-Lab have been found at pH=5.2, which are consistent with the values reported in literature [48]. The dashed lines delimit the ranges were  $|\zeta| > 30$  mV, generally considered as stability zones for the materials studied here [7][49] where the agglomeration state is minimum and the suspension stability is maximum: the electrostatic repulsion between particles is sufficiently strong to avoid or limit agglomeration phenomena. We should note here that the zeta potential values measured at 0.1 M ionic strength are lower than expected ones in the particle suspension in ultrapure water due to the strong compression of the diffuse layer at high salt content inducing a reduction of the electric potential at the slipping surface. But, in these conditions the IEP remains unchanged whatever the ionic strength. The best way for fully stabilizing the suspension is to increase the surface charge of the nanoparticles maximizing the NP-NP repulsive interactions. By changing the pH of the suspension, the surface charge state of NP can thus be adjusted.

The stability range is reached for pH > 7 and pH> 9 for TiO<sub>2</sub>-Lab and for CeO<sub>2</sub>-Lab (Figure 1), respectively. However, for pH > 9, zeta potential is negative which is not suitable for a proper deposition on a silicon substrate.

A balance must be attained between suspension stability and maximum adhesion of nanoparticles on the substrate during deposition phase. Consequently, for an optimal deposition, it has been decided to use a suspension with pH = 2, which corresponds to the maximum positive zeta potential value (+20 mV), even if this value is strictly speaking not in the stability zone.

Nanoparticles of silica used in this study (SiO<sub>2</sub>) have a negative zeta potential at initial pH of 5.3. By adding the NaOH base, the potential decreases gradually to reach a negative value of -45 mV at pH 11 passing through an isoelectric point around pH 3.

On the full pH-range explored (from 2 to 11) for TiO<sub>2</sub>-Food, zeta potential is always negative and the isoelectric point is below pH = 2. This result may seem surprising because in the literature, the isoelectric point of TiO<sub>2</sub> has been found around pH = 5-6 [48]. But TiO<sub>2</sub>-Food particles may be coated by SiO<sub>2</sub> to annihilate their surface photo-catalytic properties [50][28]. As isoelectric point of SiO<sub>2</sub> is around pH = 2 [50], it can be deduced that the particles studied here are TiO<sub>2</sub>-SiO<sub>2</sub> core-shell particles.

Briefly, adjusting the pH to a value maximizing  $|\zeta|$  for the deposition of the suspension on a substrate for SEM observations enhances the possibility of having isolated particles and minimizes the amount of agglomerates on the substrate. Another condition for a good deposition is an adequacy between the charge state at the substrate surface and the charge of the deposited particles. If the substrate surface and particles are both negatively or positively charged, the particles will not be able to adhere to the surface. The chosen substrate is a silicon wafer, which is negatively charged at the surface. So the particles must be positively charged for an optimal adhesion.

The simplest way to deposit particles for SEM observations consists in depositing a drop of the suspension on the substrate and let dry naturally with the air. This method generally leads to agglomeration of particles on the substrate and is not appropriate for observation and measurement of individual nanoparticles. As shown in our previous paper [14], a good dispersion of nanoparticles on silicon wafer can be reached using a spin-coater during the deposition. The substrate is placed on the rotating plate of the spin-coater, a drop of the particles suspension is placed on the substrate, and the deposition is made in two steps as described in materials and method section. The choice of speed and duration for the first step depends on the substrate and the solvent and they have to be adjusted to obtain an optimal deposition with well-dispersed and separated particles and limited 2D-agglomeration of particles occurring during deposition. To demonstrate the effect of spin-coating process and the impact of nanoparticle surface charge, two different suspensions of TiO<sub>2</sub>-Lab at pH=2 ( $\zeta$  = +40 mV) and pH=6 ( $\zeta$  = -5 mV), have been prepared and one droplet (7.5  $\mu$ L) of each one has been deposited following two methods of sample preparation.

SEM images of four prepared samples are reported in Figure 2; (a) pH=6 without spin-coater, (b) pH=6 with spin-coater, (c) pH=2 without spin-coater, (d) the sample prepared with the method described above at pH=2 with spin-coater.

Each suspension has been sonicated with the protocol indicated above prior to deposition. Image (a) exhibits strong 3D-agglomeration. At pH=6, zeta potential is close to point of zero charge (PZC) or iso-electric point (IEP), so agglomeration process can occur in the suspension and the sonication seems to break the agglomerates, but the step of deposit induced a re-agglomeration step. Moreover, the deposition method without spin-coater did not enable the agglomerates to be dispersed on the substrate. On image (b), 3D-agglomerates formed in the suspension at pH=6 are still present but the advantage of using the spin-coater is visible: a better dispersion was reached but numerous agglomerates remain. Image (c) demonstrates the effect of changing the pH of the suspension: particles are less agglomerated than on image (a). As a matter

of fact, the image (a) exhibits more particles layers. Nevertheless, without the spin-coater, the particles are not dispersed and separated on the substrate. Finally, image (d) shows the result of the combination of a pH change and the use of a spin-coater: as expected, due to the pH change, an important proportion of particles are isolated, only a limited number of small agglomerates remain, and the use of the spin-coater enabled the particles to be well-dispersed on the substrate surface. Consequently, image (d) is much more suitable for counting and measuring constituent particles and the evaluation of the size distribution of the particles population.

Initially the same protocol than TiO<sub>2</sub>-Lab should have been applied for TiO<sub>2</sub>-Food. But the surface charge is negative (the isoelectric point, IEP, ≈ 2), see Figure 1. Thus, for TiO<sub>2</sub>-Food and SiO<sub>2</sub>, the charge changes being impossible by modifying the pH, the protocol has to be adapted. So, the charge of the substrate surface has been changed by applying on it a fine layer of Poly-L-Lysine (PLL). In opposite, Figure 1 shows that the CeO<sub>2</sub>-Lab nanoparticles have an isoelectric point, IEP, ≈ 5 similar to TiO<sub>2</sub>-Lab. Consequently, the deposit of the CeO<sub>2</sub>-Lab colloidal suspension could be done on silica wafer without PLL. For the deposition, all suspensions have been sonicated with the probe-sonicator with the same parameters as used for TiO<sub>2</sub>-Lab. A drop of suspension with negative zeta potential (SiO<sub>2</sub> and TiO<sub>2</sub>-Food with silica coating) has been deposited on a silicon substrate covered with a fine layer of PLL by spin-coating with the same parameters as those used for TiO<sub>2</sub>-Lab (Fig.2). An example of image is shown on Figure 3.

Results indicate that concerning two types of TiO<sub>2</sub> (Fig.3 a and b), the dispersion of particles on SEM images reaches an optimum with a maximal fraction of isolated nanoparticles. On the SEM images it is possible to distinguish isolate and agglomerated particles. To obtain a more quantitative data, the SEM images were analyzed to determine the particle size distribution. Only isolated particles have been selected by the user and measured by Platypus software. The total number of measured particles was 436. As the particles are not spherical, the measured diameter is an area-equivalent diameter, D<sub>area-eq</sub>. Then, the histogram of the size distribution of the population has been established and is shown on Figure 4.

On opposite on the SEM pictures from CeO<sub>2</sub>-Lab or SiO<sub>2</sub> (Fig.3 c and d), large agglomerates are visible and no isolated particles are present although the difference of charge between particle and substrate is favorable for a better adhesion of particles. In this case, the observed behaviour is probably due to an initial suspension composed of many aggregates. Thus, the sonication process described in the previous section is not strong enough to break the agglomerates consisting of small nanoparticles with sizes smaller than 20 nm as seen in Figure 3.

The state of agglomeration/aggregation of CeO<sub>2</sub>-Lab and SiO<sub>2</sub> as seen in Fig. 3 could originate from initial state of the colloidal suspension. The difference of behavior observed in Fig.3 between both TiO<sub>2</sub> nanoparticles and the CeO<sub>2</sub>-Lab or SiO<sub>2</sub> particles could be explained by their different physico-chemical properties. The agglomerates/aggregates are originally present in the powder. That is the reason why, it is often difficult to obtain a suspension with isolated particles when a powder is re-suspended in a solvent. In

the case of CeO<sub>2</sub>-Lab and SiO<sub>2</sub> even after a sonication phase of the suspension, the nanosized constituent particles the most rigidly bounded are not easily dispersible.

Indeed, for instance, the destabilization of a colloidal suspension can be monitored by measuring the changes of measured hydrodynamic diameter by DLS over time due to the emergence of agglomeration process [51] (see section Materials and Methods).

For CeO<sub>2</sub>-Lab and SiO<sub>2</sub>, the sample preparation protocol has to be adapted taking into account the influence of the ultrasonic energy by applying ultra-sonication probe with amplitude fixed at 20%, 30% or 40%. The effectiveness of the applied sonication conditions (energy and cycles) was evaluated by measuring the evolution of the hydrodynamic diameter after ultra-sonication during 20 or 60 minutes. In principle, the reduction of the hydrodynamic diameter indicates a decrease of agglomeration state and a better effective dispersion. The best results have obtained at 1 667 J/mL probe sonication energy (amplitude 40 %) for SiO<sub>2</sub>. The hydrodynamic diameter is minimal and reaches roughly 200 nm. Moreover, this value remains stable over the full measuring time. Regarding CeO<sub>2</sub>-Lab, the amplitude of 40% seems also required and the minimum mean hydrodynamic diameter (number weighted) has been found to be nearly 50 nm. However, the reduction of the size is less significant and the measurements exhibit a behavior more fluctuating than in the case of SiO<sub>2</sub> particles demonstrating a likely dynamic process of agglomeration/sedimentation linked to the high density of CeO<sub>2</sub> particles.

The energy value defined as optimum for each kind of particles is fixed at 1 667 J/mL and sonication cycles were modified to further break down agglomerates. The Figure 6 presents the effects of direct application of pulse sonication on agglomeration kinetics of particles (SiO<sub>2</sub> and CeO<sub>2</sub>-Lab) and on decreases of the agglomerate size.

Decreasing the cycle time (10 s ON and 10 s OFF) promotes clearly the desagglomeration of silica particles (Fig. 6 a). The effects of the ultra-sonication force with an amplitude fixed at 40% on SiO<sub>2</sub> agglomerates generate a better breakage of the linked particles through a combined effect of reduction of cycle time and increasing of the number of the pulses cycles. In contrast, regarding CeO<sub>2</sub>-Lab particles, no significant differences were noticed by changing the couple of pulses (Fig. 6 b).

Duration time of sonication should have an impact on the reduction of particle agglomeration as well [41]. This parameter has been modified in Figure 7 and the combination of time duration and pulses of ultra-sonication shows a clear trend in the agglomerate breakage, only for SiO<sub>2</sub> particles.

As a conclusion, faster cycles of pulses (10 s ON and 10 s OFF) coupled with the maximal amplitude (40 %) and a total measuring time of 20 nm lead to a more stable and homogeneous colloidal suspension without re-agglomeration process.

Samples have been prepared following this protocol of re-dispersion. Suspensions of CeO<sub>2</sub>-Lab (pH = 2) and SiO<sub>2</sub> (pH=8) have been sonicated with new parameters for the probe sonicator. A drop of the CeO<sub>2</sub>-Lab and SiO<sub>2</sub> suspension has been deposited on a silicon substrate with the spin-coater (spreading phase: 60 s at 1 000 rpm, drying phase: 10 s at 8 000 rpm). Regarding CeO<sub>2</sub>-Lab, note that the deposition has been made just after the sonication in order to limit agglomeration process between sonication step and deposition (a zeta potential is not sufficiently high to guarantee the stability of the suspension over time). The silicon wafer has been functionalized with PLL prior to depositing SiO<sub>2</sub> particles because it is not possible to make positive the surface charge of these particles with adjusting high zeta potential from Figure 1.

Then, SEM images were performed to visualize particles morphological features and determine their size (Figures 8 and 9). Furthermore, SEM images obtained with the initial parameters are reported in Figure 8a) and 9a) in order to demonstrate the impact of optimized re-dispersion protocol on the agglomerate size. For these new sonication parameters, SEM images show silica nanoparticles aggregates with an average size around 150 nm. Compact aggregates are composed of SiO<sub>2</sub> constituent nanoparticles corresponding to a D<sub>area-eq.</sub> at around 18 nm (see figure 8). These aggregates measured by DLS present a mean hydrodynamic diameter D<sub>hd</sub> equal to 145.6 nm ± 10.4nm corresponding to the maximal size reduction of aggregates observed by SEM. Consequently, the DLS and SEM measurements are consistent.

SEM images of the aggregates of the CeO<sub>2</sub>-Lab nanoparticles with modified sonication cycles are shown in Figure 9. The CeO<sub>2</sub>-Lab formed anisometric aggregates (Fig. 9 a). Here again, the aggregate size evaluated by SEM seems to be very close to hydrodynamic diameter measurements performed by DLS ranging from 50 to 100 nm.

The various images obtained by SEM are suitable for building histogram of the size distribution of particles using Platypus software. The histograms of both NP populations are shown in Figure 10. Only constituent nanoparticle within each aggregate has been counted.

The histogram corresponding to CeO<sub>2</sub>-Lab (Fig. 10 a) has been fitted with a mixture of Log-Normal distribution with two peaks. The diameter corresponding to the first peak is D<sub>area-eq.</sub> = 9.6 nm and the size distribution is σ= 0.7 nm and the second peak is D<sub>area-eq.</sub> = 16.1 nm and the size distribution is σ = 3.5 nm.

The histogram corresponding to SiO<sub>2</sub>-Lab (Fig. 10 b) has been fitted with Log-Normal distribution. The mean diameter is D<sub>area-eq.</sub> = 15.6 nm and the size distribution is σ = 3.7 nm.

Finally to answer to the regulatory classification of nanomaterials, we have developed a methodology to analyze the size of constituent particles by SEM. The table 1 summarized relevant parameters fixed to achieve to an optimal sonication to break the agglomerates consisting in small nanoparticles and dispersed on a substrate for SEM imaging technique.

## **Conclusion**

This paper proposes an improvement of sample preparation and validation of a protocol for size measurements of nanoparticles in suspension, powder or extracted from complex media by SEM. We have examined the feasibility of combining several factors such as pH, zeta potential, temperature, duration and power of sonication, concentration and spin coater parameters, that can influence electrostatic interactions and agglomeration of nanoparticles. As expected, the state of agglomeration/aggregation of particles in colloidal suspension seems depends on their different physico-chemical properties and behavior. The agglomerates originally present in particles powder form re-suspended in a solvent seems exacerbated when the initial particles are small.

This paper has shown that ultra-sonication process of colloidal suspension of TiO<sub>2</sub> nanoparticles (synthesized or extracted from food products) with a low initial agglomeration state has been improved by applying a sonication amplitude fixed at 20% with cycles (10s, 30s) corresponding to an ultrasonic dispersion energy value of 378 J/mL. This optimized process leads to a final dispersion with maximal isolated particles. For the other agglomerate powders (e.g. silica and cerium dioxide), the optimal dispersion level is reached when the dispersion energy value is higher (1 667 J/mL) and combined with faster cycles of pulses (10s, 10s). This optimization of power parameters has been carried out by monitoring by DLS the reduction of agglomerate sizes.

Sonication step is a crucial point to have a maximal small aggregates and a stable colloidal suspension. Our results highlight that sonication protocol leads to significant reductions in the agglomerate size. The agglomeration state and the stability of the colloidal suspension over time can be measured and monitored by using DLS technique. This makes it possible to adjust the parameters to prepare a suitable colloidal suspension for a deposition by spin-coater and SEM analysis. The challenge consisting in evaluating the size measurement of the constituent particles in accordance with the regulation has been carried out successfully.

## **Acknowledgement**

The authors are grateful to A. Allard from LNE for statistical support.

## Reference

- [1] I. De la Calle, M. Menta, F. Séby, Current trends and challenges in sample preparation for metallic nanoparticles analysis in daily products and environmental samples: A review, *Spectrochim. Acta Part B At. Spectrosc.* (2016) 125: 66–96. doi:10.1016/j.sab.2016.09.007.
- [2] T.A.J. Kuhlbusch, S.W.P. Wijnhoven, A. Haase, Nanomaterial exposures for worker, consumer and the general public, *NanoImpact*. (2018) 10: 11–25. doi:10.1016/j.impact.2017.11.003.
- [3] European Commission, Commission Recommendation of 18 October 2011, on the definition of nanomaterial (2011/696/EU). *Official J. Eur.Union* (2011) 54: 38-40. doi:10.3000/18770677.L\_2011.275.eng
- [4] ISO/TR 13014:2012 Nanotechnologies : Guidance on physico-chemical characterization of engineered nanoscale materials for toxicologic assessment (2012). <https://www.iso.org/obp/ui/#iso:std:iso:tr:13014:ed-1:v1:fr>.
- [5] M. Mayne-L’Hermite, R. Tantra, I. Romer, M. Carriere, E. Valsami-Jones, L.-J. Ellis, S. Allard, I. Kaur, W. Unger, S. Rades, A. Potthoff, C. Minelli, Dispersion of Nanomaterials in Aqueous Media: Towards Protocol Optimization, *J. Vis. Exp.* (2017) Dec 25;(130). doi:10.3791/56074.
- [6] V.P.J. Bautista, K. Klaus, H. Uwe, W. Wendel, K. Thomas, B. Alison, M. Greg, H.-G. Angelika, K. Stefan, R. Martin, G. Douglas, G. Peter, S.-K. Birgit, S. Hermann, L. Heike, Basic comparison of particle size distribution measurements of pigments and fillers using commonly available industrial methods, *JRC Technical reports Report EUR 26916 EN* (2014). doi:10.2788/21024.
- [7] N. Mandzy, E. Grulke, T. Druffel, Breakage of TiO<sub>2</sub> agglomerates in electrostatically stabilized aqueous dispersions, *Powder Technol.* (2005) 160: 121–126. doi:10.1016/j.powtec.2005.08.020.
- [8] J.S. Taurozzi, V.A. Hackley, M.R. Wiesner, Ultrasonic dispersion of nanoparticles for environmental, health and safety assessment – issues and recommendations, *Nanotox.* (2011) 5: 711–729. doi:10.3109/17435390.2010.528846.
- [9] M. Pohl, H. Schubert, H.P. Schuchmann, Herstellung stabiler Dispersionen aus pyrogener Kieselsäure, *Chem-Ing-Tech.* (2005) 77: 258–262. doi:10.1002/cite.200407020.
- [10] J. Kim, D.F. Lawler, Jinkeun Kim and Desmond F. Lawler, Characteristics of Zeta Potential Distribution in Silica Particles, *Bull. Korean Chem. Soc.* (2005) 26: 1083–1089. doi:10.5012/bkcs.2005.26.7.1083.
- [11] J. Jiang, G. Oberdörster, P. Biswas, Characterization of size, surface charge, and agglomeration state of nanoparticle dispersions for toxicological studies., *J. Nanopart. Res.* (2009) 11: 77-89. doi:10.1007/s11051-008-9446-4.
- [12] P.A. Kralchevsky, K. Nagayama, Capillary Forces between Colloidal Particles, *Langmuir*. (1994) 10: 23–36. doi:10.1021/la00013a004.
- [13] A. Thill, O. Spalla, Aggregation due to capillary forces during drying of particle submonolayers, *Colloids Surf. A Physicochem. Eng. Aspects* (2003) 217: 143-151. doi:10.1016/S0927-7757(02)00569-1.
- [14] A. Delvallée, N. Feltin, S. Ducourtieux, M. Trabelsi, J.F. Hochepied, Direct comparison of AFM and SEM measurements on the same set of nanoparticles, *Meas. Sci. Technol.* (2015) 26: 85601. doi:10.1088/0957-0233/26/8/085601.
- [15] C. M. Hoo, T. Doan, N. Starostin, P. West, M. Mecartney, Optimal sample preparation for nanoparticle metrology (statistical size measurements) using atomic force microscopy, *J. Nanopart.*

Res (2010) 12: 939–949. doi:10.1007/s11051-009-9644-8.

- [16] R.D. Boyd, S.K. Pichaimuthu, A. Cuenat, New approach to inter-technique comparisons for nanoparticle size measurements; using atomic force microscopy, nanoparticle tracking analysis and dynamic light scattering, *Colloids Surf. A Physicochem. Eng. Aspects* (2011) 387: 35–42. doi:10.1016/j.colsurfa.2011.07.020.
- [17] I. De la Calle, M. Menta, F. Séby, Current trends and challenges in sample preparation for metallic nanoparticles analysis in daily products and environmental samples: A review, *Spectrochim. Acta - Part B At. Spectrosc.* (2016) 125: 66–96. doi:10.1016/j.sab.2016.09.007.
- [18] P.J. Lu, W.E. Fu, S.C. Huang, C.Y. Lin, M.L. Ho, Y.P. Chen, H.F. Cheng, Methodology for sample preparation and size measurement of commercial ZnO nanoparticles, *J. Food Drug Anal.* (2018) 26: 628–636. doi:10.1016/j.jfda.2017.07.004.
- [19] I. de la Calle, M. Menta, M. Klein, F. Séby, Study of the presence of micro- and nanoparticles in drinks and foods by multiple analytical techniques, *Food Chem.* (2018) 266: 133–145. doi:10.1016/j.foodchem.2018.05.107.
- [20] I. de la Calle, M. Menta, M. Klein, F. Séby, Screening of TiO<sub>2</sub> and Au nanoparticles in cosmetics and determination of elemental impurities by multiple techniques (DLS, SP-ICP-MS, ICP-MS and ICP-OES), *Talanta*. (2017) 17: 291–306. doi:10.1016/j.talanta.2017.05.002.
- [21] F. Babick, J. Mielke, W. Wohlleben, S. Weigel, V.D. Hodoroaba, How reliably can a material be classified as a nanomaterial? Available particle-sizing techniques at work, *J. Nanopart. Res.* (2016) 18: 158. doi:10.1007/s11051-016-3461-7.
- [22] R. Brügel, J. Rückert, W. Wohlleben, F. Babick, A. Ghanem, C. Gaillard, A. Mech, H. Rauscher, S. Weigel, C. Friedrich, The NanoDefiner e-tool — A decision support framework for recommendation of suitable measurement techniques for the assessment of potential nanomaterials, IEEE 12<sup>th</sup> Nanomaterials and Devices Conference (NMDC 2017), Singapore, 02.-04.10.2017, pp.71-72; doi:10.1109/NMDC.2017.8350509.
- [23] T. Usimäki, P. Hallegot, Protocols for preparation of products for microscopy methods- NanoDefine Technical Report D2.4, The NanoDefine Consortium Wageningen, 2016. <http://www.nanodefine.eu/index.php/downloads/public-deliverables>
- [24] P. Brüning, Review and practical evaluation of sampling guidelines-NanoDefine Technical Report D2.7, The NanoDefine Consortium 2017. <http://www.nanodefine.eu/index.php/downloads/public-deliverables>
- [25] M.E. Vance, T. Kuiken, E.P. Vejerano, S.P. McGinnis, M.F.H. Jr, D. Rejeski, M.S. Hull, Nanotechnology in the real world : Redeveloping the nanomaterial consumer products inventory, *Beilstein J. Nanotechnol.* (2015) 6: 1769–1780. doi:10.3762/bjnano.6.181.
- [26] R. Peters, P. Brandhoff, S. Weigel, H. Marvin, H. Bouwmeester, K. Aschberger, H. Rauscher, V. Amenta, M. Arena, F. Botelho Moniz, S. Gottardo, A. Mech, Inventory of Nanotechnology applications in the agricultural, feed and food sector, *EFSA Support. Publ.* 11 (2017). doi:10.2903/sp.efsa.2014.en-621.
- [27] M.-H. Ropers, H. Terrisse, M. Mercier-Bonin, B. Humbert, Titanium Dioxide as Food Additive, *Appl. Titan. Dioxide* (2017) Chap. 1, intechOpen. doi:10.5772/intechopen.68883.
- [28] R.J.B. Peters, G. van Bemmel, Z. Herrera-Rivera, H.P.F.G. Helsper, H.J.P. Marvin, S. Weigel, P.C. Tromp, A.G. Oomen, A.G. Rietveld, H. Bouwmeester, Characterization of Titanium Dioxide Nanoparticles in Food Products: Analytical Methods To Define Nanoparticles, *J. Agric. Food Chem.* (2014) 62: 6285–6293. doi:10.1021/jf5011885.

- [29] S. Das, J.M. Dowding, K.E. Klump, J.F. McGinnis, W. Self, S. Seal, Cerium oxide nanoparticles: Applications and prospects in nanomedicine, *Nanomed.* (2013) 8: 1483–1508. doi:10.2217/nmm.13.133.
- [30] V. Sajith, C.B. Sobhan, G.P. Peterson, Experimental investigations on the effects of cerium oxide nanoparticle fuel additives on biodiesel, *Adv. Mech. Eng.* (2010) 3: 1-6. doi:10.1155/2010/581407.
- [31] M. Marchetti (2013), Design, synthesis and chemical-physical characterization of photocatalytic inorganic nanocrystals for innovative technological applications, PhD thesis, Università degli Studi di Bologna. [http://amsdottorato.unibo.it/5737/2/marchetti\\_marco\\_tesi.pdf](http://amsdottorato.unibo.it/5737/2/marchetti_marco_tesi.pdf) (accessed December 20, 2013).
- [32] O.E. I. Florea, C. Feral-Martin, J. Majimel, D. Ihiawakrim, C. Hirlimann, Three-dimensional tomographic analyses of CeO<sub>2</sub> nanoparticles, *Cryst. Growth Des.* (2013) 13: 1110-1121. <https://doi.org/10.1021/cg301445h>
- [33] X.-X. Chen, B. Cheng, Y.-X. Yang, A. Cao, J.-H. Liu, L.-J. Du, Y. Liu, Y. Zhao, H. Wang, Characterization and Preliminary Toxicity Assay of Nano-Titanium Dioxide Additive in Sugar-Coated Chewing Gum, *Small.* (2013) 9: 1765–1774. doi:10.1002/smll.201201506.
- [34] R.R. Retamal Marín, F. Babick, M. Stintz, Ultrasonic dispersion of nanostructured materials with probe sonication – practical aspects of sample preparation, *Powder Technol.* (2017) 318: 451–458. doi:10.1016/j.powtec.2017.05.049.
- [35] K.A. Jensen, H. Crutzen, A. Dijkzeul, P. Office, NANoREG Guidance Document, European Commission (2015).
- [36] R. Retamal Marín, F. Babick, G.-G. Lindner, M. Wiemann, M. Stintz, Effects of Sample Preparation on Particle Size Distributions of Different Types of Silica in Suspensions, *Nanomat.* (2018) 8: 454. doi:10.3390/nano8070454.
- [37] N. Feltin, L. Devoille, G. Favre, S. Artous, J.-F. Hochepied, Development of reference measurement methods to support SME in the implementation of a metrological characterization of nanomaterials. NANOMET project, *Spectra Analyse Journal* (2016).
- [38] M.T. and J.F.H. A Delvallée, N Feltin, S Ducourtieux, Toward an uncertainty budget for measuring nanoparticles by AFM, *Metrologia.* 53 (2015). doi:10.1088/0026-1394/53/1/41.
- [39] L. Crouzier, A. Delvallée, S. Ducourtieux, S, L. Devoille, G. Noircler, C. Ulysse, O.Taché, E. Barruet, C. Tromas, N. Feltin, Development of a new hybrid approach combining AFM and SEM for the nanoparticle dimensional metrology, *Beilstein J. Nanotechnol.* (2019), 10: 1523-1536. doi:10.3762/bjnano.10.150
- [40] M.J.S. D.Mott, B.Cotts, I-IM S, J.Luo, H.-Y. Park, P. N. Njoki, Size Determination of Nanoparticles Based on Tapping-Mode Atomic Force Microscopy Measurements, *J. Scann. Probe Microsc* (2008), 3: 1–8. <https://doi.org/10.1166/jspm.2008.001>.
- [41] I. Kaur, L.-J. Ellis, I. Romer, R. Tantra, M. Carriere, S. Allard, M. Mayne-L’Hermite, C. Minelli, W. Unger, A. Potthoff, S. Rades, E. Valsami-Jones, Dispersion of Nanomaterials in Aqueous Media: Towards Protocol Optimization, *J. Vis. Exp.* (2017), (130), e56074. doi:10.3791/56074.
- [42] S. Pradhan, J. Hedberg, E. Blomberg, S. Wold, I. Odnevall Wallinder, Effect of sonication on particle dispersion, administered dose and metal release of non-functionalized, non-inert metal nanoparticles, *J. Nanoparticle Res.* (2016) 18: 285. doi:10.1007/s11051-016-3597-5.
- [43] F. Varenne, J. Botton, C. Merlet, M. Beck-Broichsitter, F.X. Legrand, C. Vauthier, Standardization and validation of a protocol of size measurements by dynamic light scattering for monodispersed

stable nanomaterial characterization, *Colloids Surfaces A Physicochem. Eng. Asp.* (2015) 486: 124–138. doi:10.1016/j.colsurfa.2015.08.043.

- [44] R.R. Retamal Marín, F. Babick, L. Hillemann, Zeta potential measurements for non-spherical colloidal particles – Practical issues of characterisation of interfacial properties of nanoparticles, *Colloids Surfaces A Physicochem. Eng. Asp.* (2017) 532: 516–521. doi:10.1016/j.colsurfa.2017.04.010.
- [45] S. Chakraborty, An investigation on the long-term stability of TiO<sub>2</sub> nanofluid, *Mater. Today Proc.* (2019) 11: 714–718. doi:10.1016/J.MATPR.2019.03.032.
- [46] C.-P. Tso, C.-M. Zhung, Y.-H. Shih, Y.-M. Tseng, S.-C. Wu, R.-A. Doong, Stability of metal oxide nanoparticles in aqueous solutions, *Water Sci. Technol.* (2010) 61: 127-133. doi:10.2166/wst.2010.787.
- [47] D. Sun, S. Kang, C. Liu, Q. Lu, L. Cui, B. Hu1, Effect of Zeta Potential and Particle Size on the Stability of SiO<sub>2</sub> Nanospheres as Carrier for Ultrasound Imaging Contrast Agents, *Int. J. Electrochem. Sci.* (2016) 11: 8520–8529. doi:10.20964/2016.10.30.
- [48] M. Kosmulski, Compilation of PZC and IEP of sparingly soluble metal oxides and hydroxides from literature, *Adv. Colloid Interface Sci.* (2009) 152: 14–25. doi:10.1016/j.cis.2009.08.003.
- [49] C. Sentein, B. Guizard, S. Giraud, C. Yé, F. Ténégé, Dispersion and stability of TiO<sub>2</sub> nanoparticles synthesized by laser pyrolysis in aqueous suspensions, *J. Phys. Conf. Ser.* (2009) 170: 4–11. doi:10.1088/1742-6596/170/1/012013.
- [50] W. Dudefou, (2017), Titanium dioxide particles in food : characterization, fate in digestive fluids and impact on human gut microbiota, PhD thesis, Université de Nantes, INRA UR1268 Biopolymères Interactions Assemblages.
- [51] F. Varenne, J. Botton, C. Merlet, H. Hillaireau, F.X. Legrand, G. Barratt, C. Vauthier, Size of monodispersed nanomaterials evaluated by dynamic light scattering: Protocol validated for measurements of 60 and 203 nm diameter nanomaterials is now extended to 100 and 400 nm, *Int. J. Pharm.* (2016) 515: 245–253. doi:10.1016/j.ijpharm.2016.10.016.

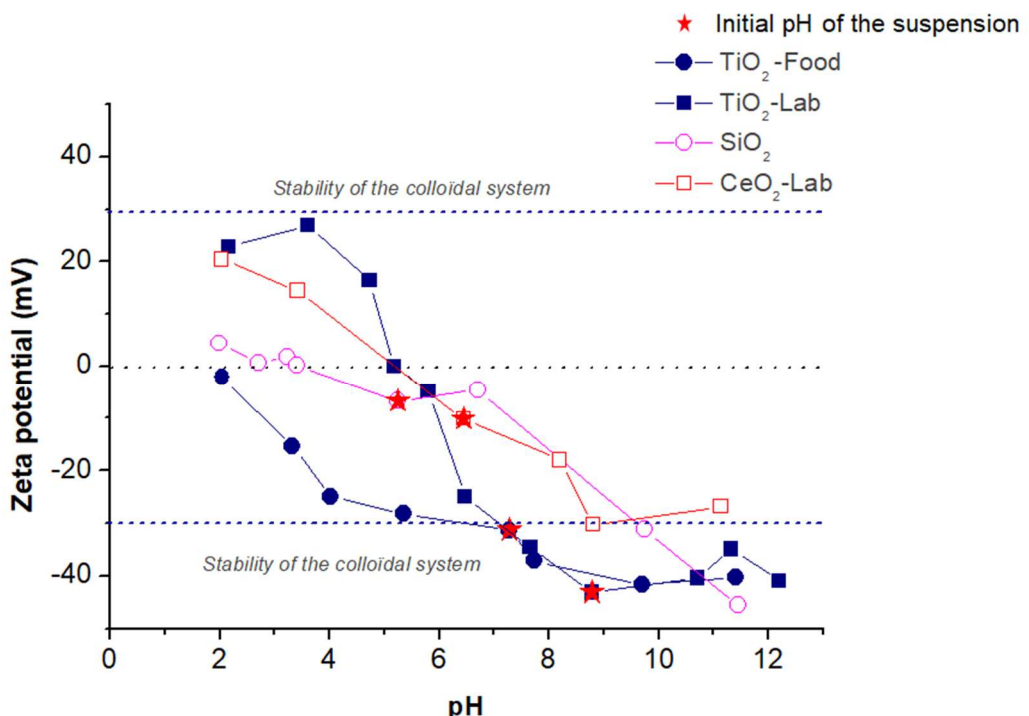


Figure 1: Zeta potential of nanoparticles as a function of pH for a suspension

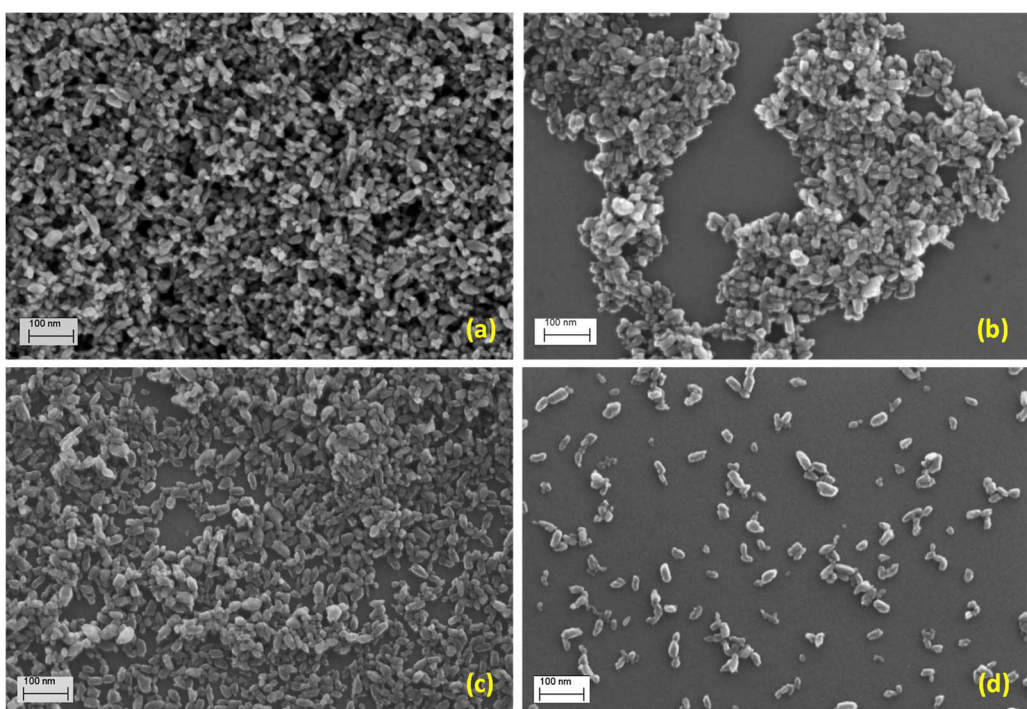


Figure 2: SEM images of TiO<sub>2</sub>-Lab nanoparticles on samples prepared with different methods. (a) At pH=6 without using the spin coater for the deposition. (b) At pH=6 with using the spin coater. (c) At pH=2 without using the spin coater. (d) At pH=2 with using the spin coater.

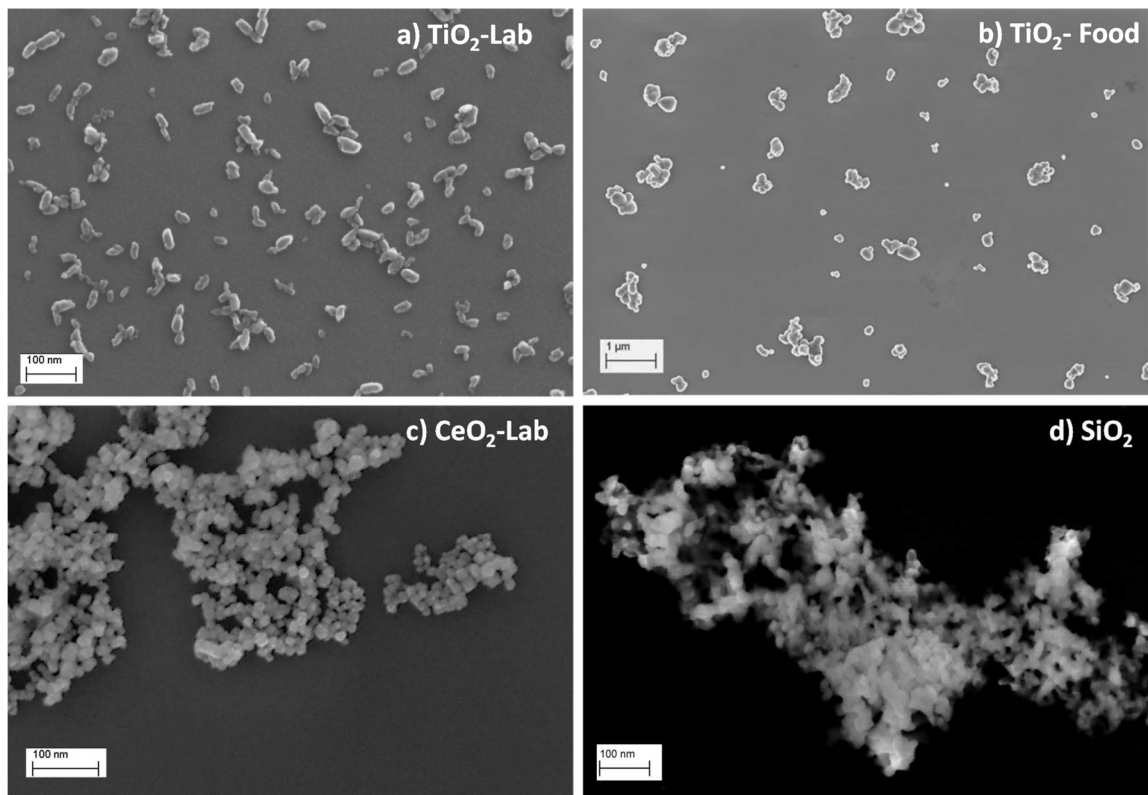
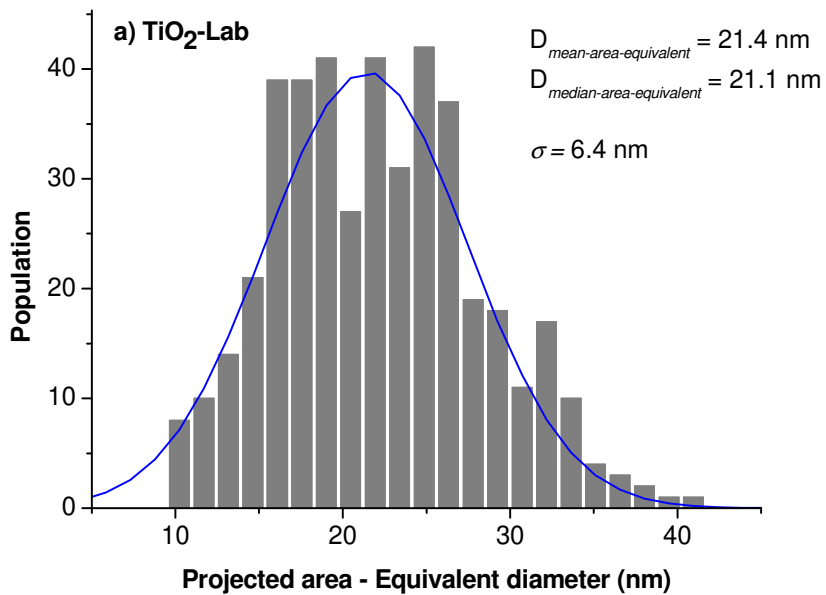
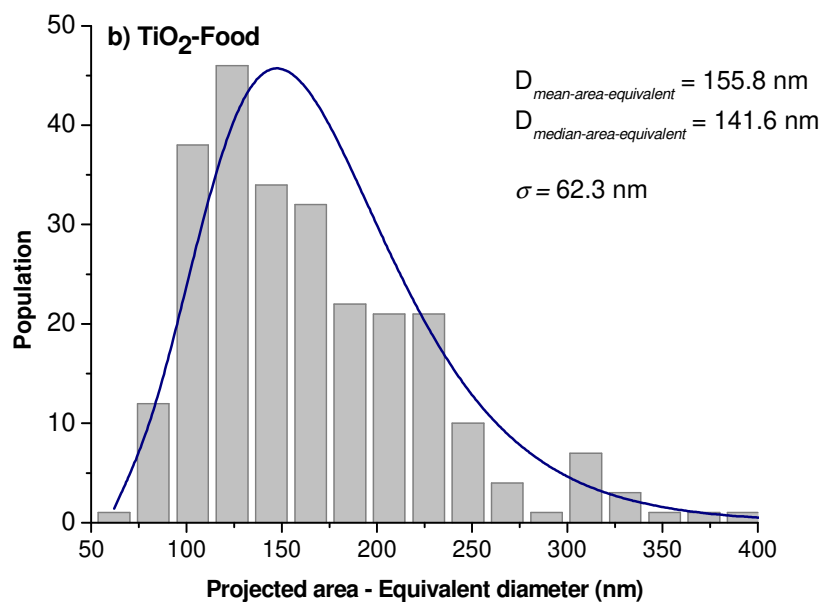


Figure 3: (a) SEM image of TiO<sub>2</sub>-Lab deposited on a silicon substrate at pH=2 with using the spin coater (*refer to Figure 2d*) (b) SEM image of TiO<sub>2</sub>-Food deposited by spin-coating on a silicon substrate covered with a PLL layer at pH = 7.3, (c) SEM image of CeO<sub>2</sub>-Lab deposited by spin-coating on a silicon substrate without a PLL layer at pH=2 and (d) SEM image of SiO<sub>2</sub> deposited by spin-coating on silicon wafer with a PLL layer at originate pH.

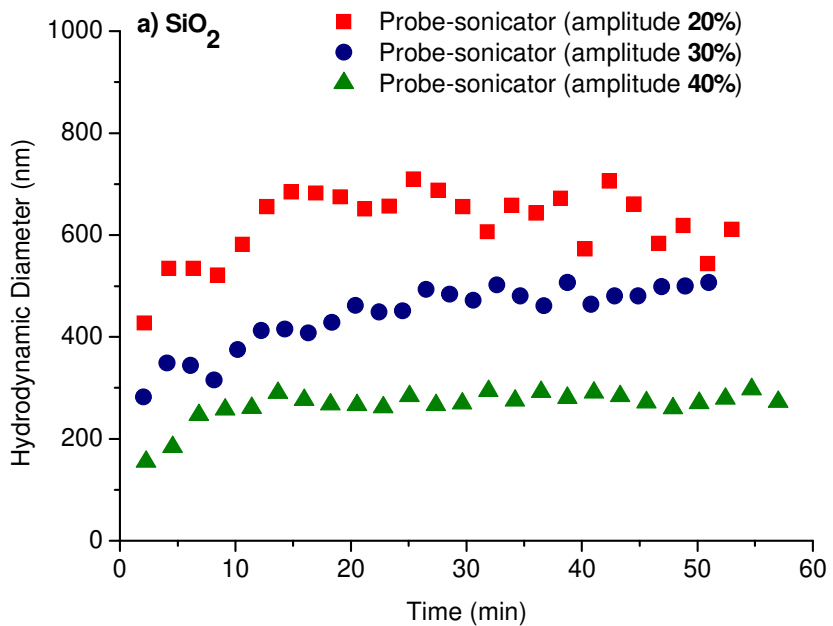


(a)

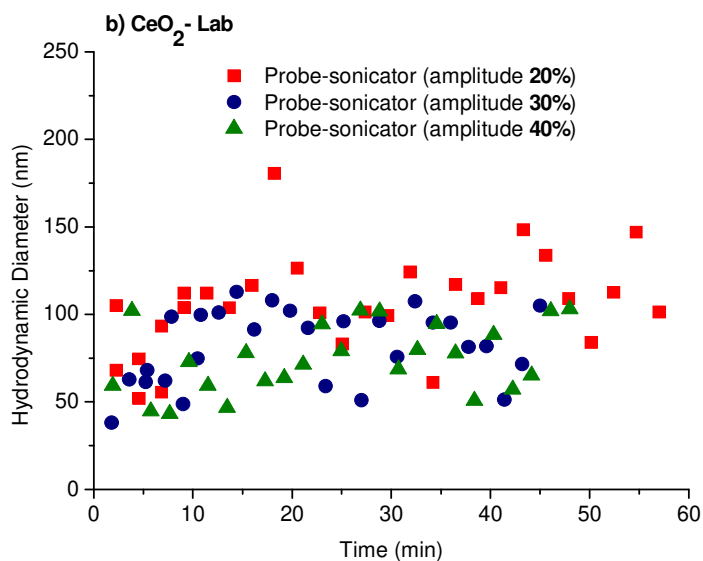


(b)

Figure 4: (a) Histogram of the size distribution of TiO<sub>2</sub>-Lab nanoparticles, fitted with a Log-Normal distribution (mean diameter  $D_{mean-area-eq.} = 21.4 \text{ nm}$ , median diameter  $D_{median-area-eq.} = 21.1 \text{ nm}$  and standard deviation  $\sigma = 6.4 \text{ nm}$ ) and (b) Histogram of the size distribution of TiO<sub>2</sub>-Food nanoparticles, fitted with a log-normal distribution (mean diameter  $D_{mean-area-eq.} = 155.8 \text{ nm}$ , median diameter  $D_{median-area-eq.} = 141.6 \text{ nm}$  and size distribution  $\sigma = 62.3 \text{ nm}$ ).



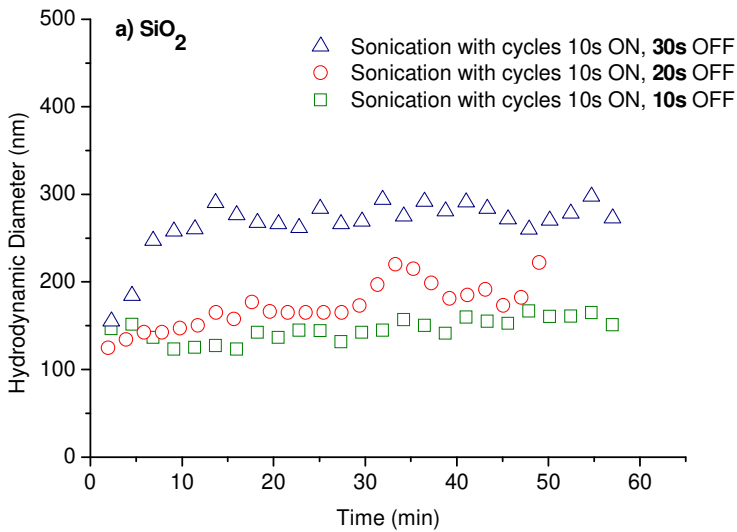
(a)



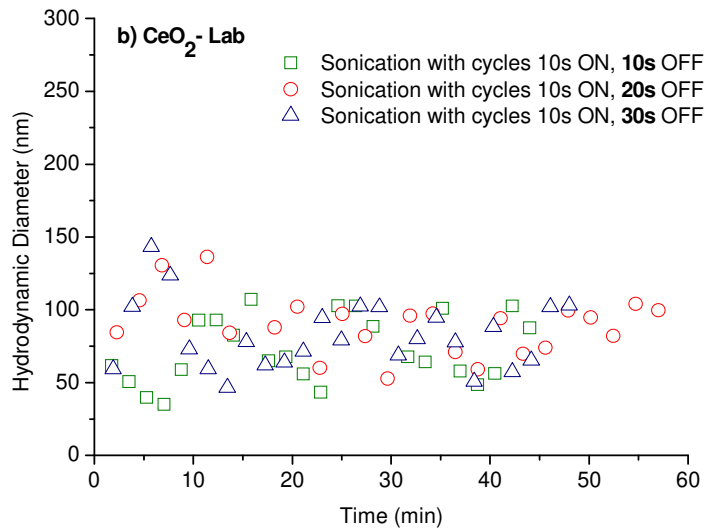
(b)

Figure 5: Evolution of the mean hydrodynamic diameter as a function of time after 20 minutes of sonication with cycles of 10 seconds ON with various amplitudes (20%, 30% or 40%) and various calorimetric energies density (378, 766 and 1667 J/mL) and then 30 seconds OFF, for

(a)  $\text{SiO}_2$  ( $\text{pH}=8$ ) and (b)  $\text{CeO}_2$ -Lab ( $\text{pH}=2$ )

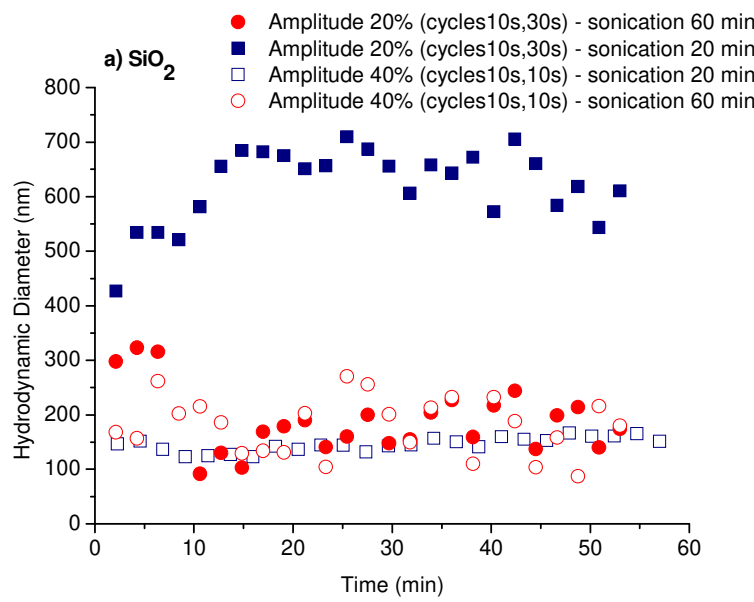


(a)

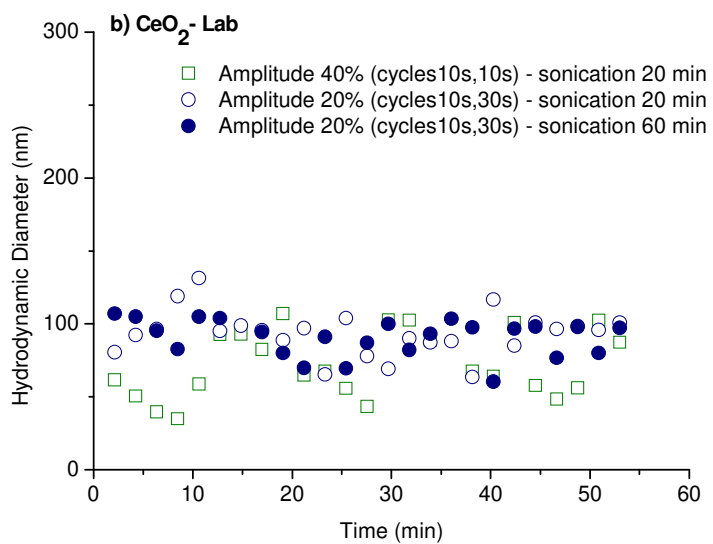


(b)

Figure 6: Evolution of the mean hydrodynamic diameter as a function of time after 20 minutes of sonication with cycles of 10 seconds ON and 10, 20 or 30 seconds OFF, for (a)  $\text{SiO}_2$  ( $\text{pH}=8$ ) and (b)  $\text{CeO}_2$ -Lab ( $\text{pH}=2$ ) with amplitude fixed at 40% in both cases



(a)



(b)

Figure 7: Evolution time of the hydrodynamic diameter according duration time of sonication, for (a)  $\text{SiO}_2$  ( $\text{pH}=8$ ) and (b)  $\text{CeO}_2$ -Lab ( $\text{pH}=2$ )

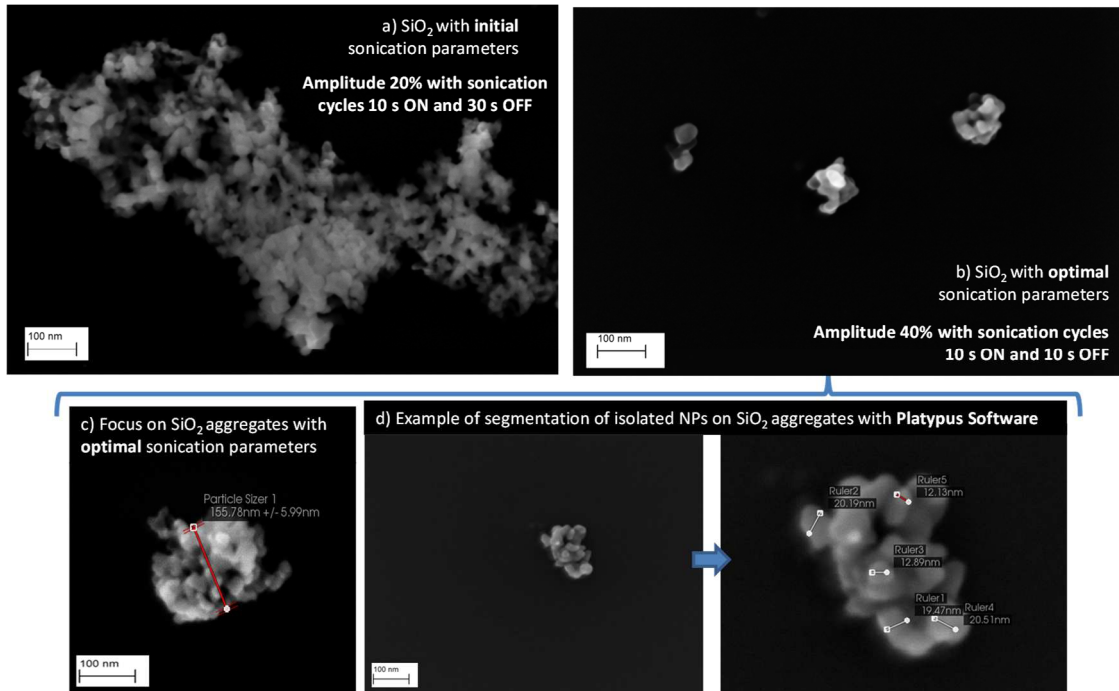


Figure 8: SEM image of SiO<sub>2</sub> deposited at initial pH on silicon wafer coated with PLL after **20 minutes of sonication** (a) at initial sonication parameters (Amplitude, 20% with cycles (10s, 30s)), (b) with **optimized sonication parameters (Amplitude, 40% with cycles (10 s, 10 s))**, (c) and (d) focus on SiO<sub>2</sub> aggregates after optimal sonication

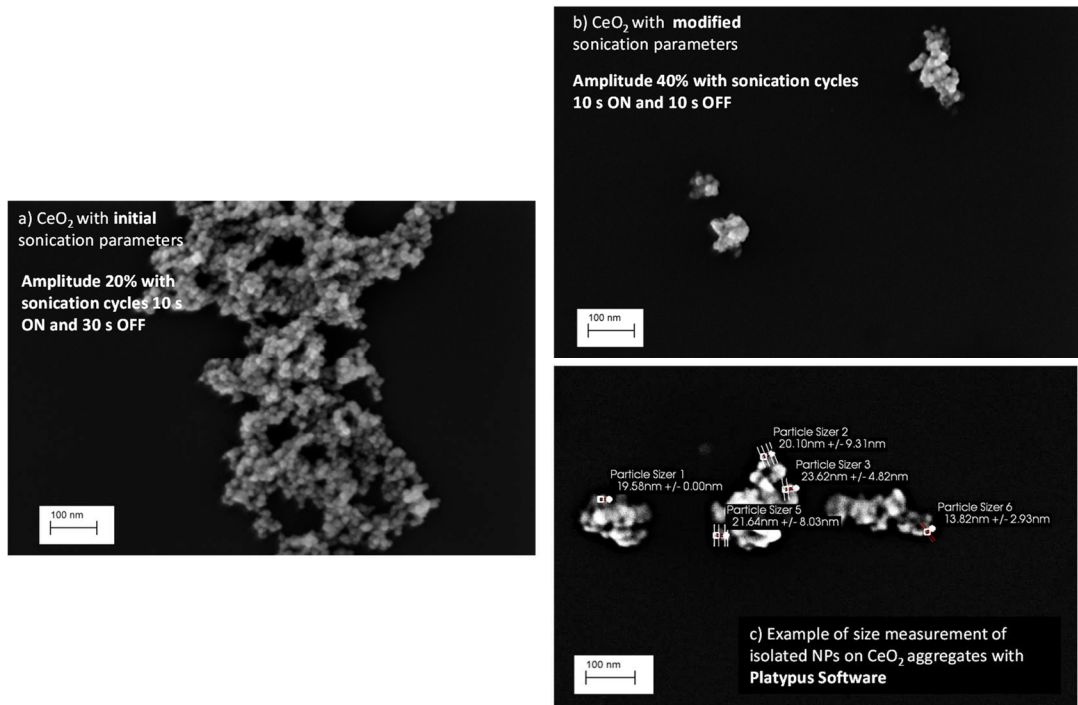
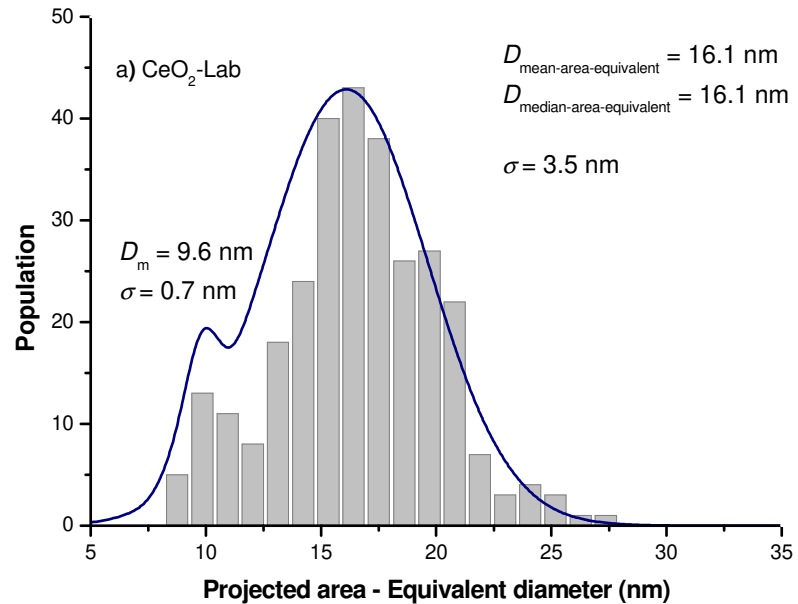
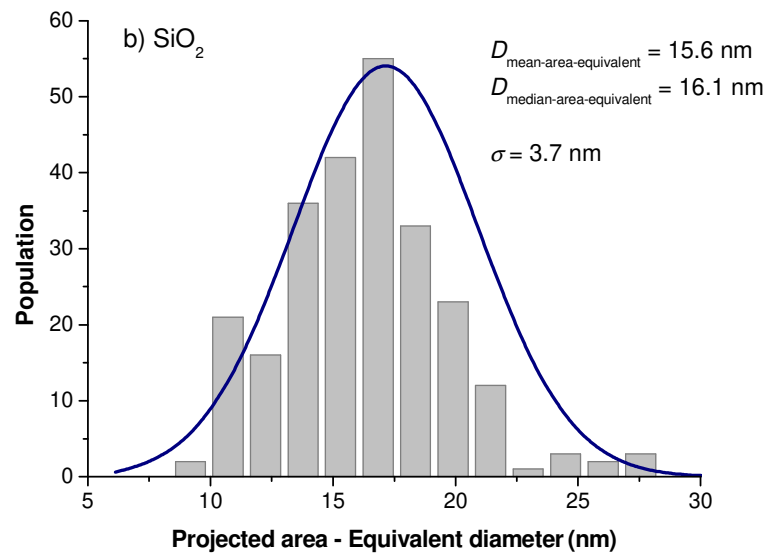


Figure 9: SEM image of CeO<sub>2</sub> deposited at pH 2 on silicon wafer after 20 minutes of sonication (a) (Amplitude, 20% with cycles (10s, 30s)), (b) with modified sonication parameters (Amplitude, 40% with cycles (10 s, 10 s)), (c) focus on CeO<sub>2</sub> aggregates after optimal sonication



(a)



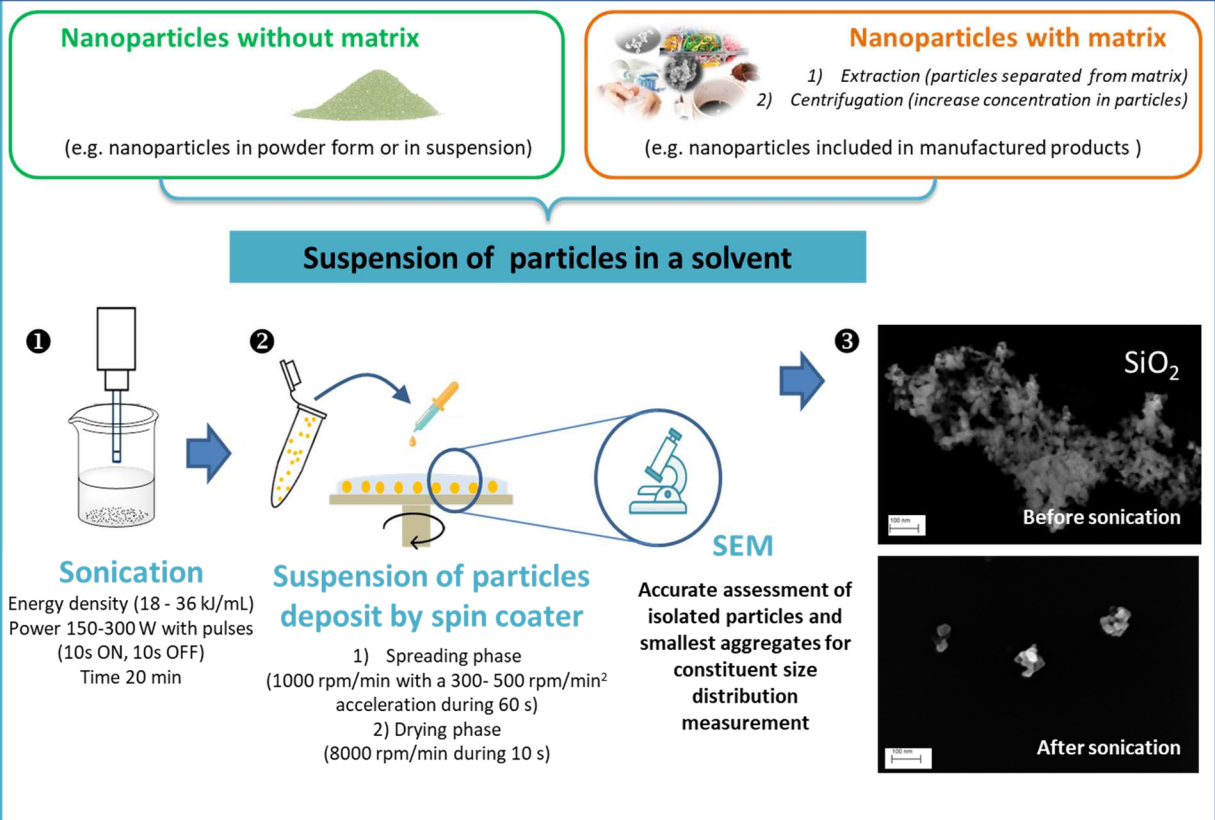
(b)

Figure 10: (a) Histogram of the size distribution of  $\text{CeO}_2\text{-Lab}$  nanoparticles, fitted with a Mix-LogNormal distribution (mean diameter  $D_{\text{mean-area-eq.}} = 16.1 \text{ nm}$ , median diameter  $D_{\text{median-area-eq.}} = 16.1 \text{ nm}$  and standard deviation  $\sigma = 6.4 \text{ nm}$ ) and (b) Histogram of the size distribution of  $\text{SiO}_2$  nanoparticles distribution (mean diameter  $D_{\text{mean-area-eq.}} = 15.6 \text{ nm}$ , median diameter  $D_{\text{median-area-eq.}} = 16.1 \text{ nm}$  and standard deviation  $\sigma = 3.7 \text{ nm}$ )

Particles	Sample Volume (mL)	Dispersing time (sonication)	Pulses	Calorimetric Energy Density (J/mL)	Number-weighted mean diameter of aggregates by DLS (nm) using NNLS method	pH	Zeta potential (mV)	Spin coater parameters	Mean diameter of constitutive particles by SEM (nm)
TiO <sub>2</sub> -Lab			10, 30	378	190	2	-43.1		21.4
TiO <sub>2</sub> -Food		300 s	10, 30	378	136	8-9 with PLL	-41.7		155.8
CeO <sub>2</sub> -Lab			10, 10	1667	72	2	-30.2		9.6 and 16.1
SiO <sub>2</sub>	10	600 s	10, 10	1667	132	8 with PLL	-42.6	Spreading phase (1000 rpm/min with a 300-500 rpm/min <sup>2</sup> acceleration during 60 s) Drying phase (8000 rpm/min during 10 s)	15.6

Table 1 : Summary of relevant parameters to access to a constitutive particle's size measured by SEM

**Method to access size distribution of constituent particles  
by Scanning Electron Microscopy**



**GRAPHICAL ABSTRACT**